Journal of Applied Fluid Mechanics, Vol. 18, No. 12, pp. 3068-3081, 2025.
Available online at www.jafmonline.net, ISSN 1735-3572, EISSN 1735-3645.
https://doi.org/10.47176/jafm.18.12.3486

Aerothermal Characteristics of Trailing Edge Region Film Cooling on a Nozzle Guide Vane

B. Gudla, and A. K. Pujari†

Mechanical engineering Department, Indian Institute of Petroleum and Energy, Visakhapatnam, Andhra Pradesh, 530003, India

†*Corresponding Author Email: arun.pujarimec@iipe.ac.in*

ABSTRACT

Maintaining the trailing edge of the first stage high-pressure nozzle guide vane (NGV) in high-temperature regions (~ 2200K) is always a challenging task compared to the other locations. This paper investigates the aero-thermal characteristics of a nozzle guide vane (NGV) with an innovative film cooling configuration to optimize cooling performance in high-temperature environments. The study examines the effects of varying blowing ratios (0.69, 1.07, 1.67, and 2.06) on total pressure losses and cooling effectiveness by replacing traditional trailing edge ejection with two rows of film-cooling holes in the post-throat region. Computational analysis using ANSYS Fluent revealed that lower blowing ratios maintain better film attachment and increase total pressure losses with an increase in the blowing ratio up to 1.67 and a drop in the losses at higher blowing ratios (2.06) due to the increasing coolant jet momentum, better mixing with the mainstream due to jet lift-off. The 20% decrease in the total pressure losses using the novel film configuration compared to the trailing edge ejection signifies the study. These findings highlight the importance of optimizing blowing ratios and hole configurations to achieve efficient cooling without compromising aerodynamic performance, providing valuable insights for designing advanced cooling systems in gas turbine engines.

Article History

Received February 28, 2025
Revised June 30, 2025
Accepted July 18, 2025
Available online October 6, 2025

Keywords:

Blowing ratio
Film cooling effectiveness
Total pressure loss coefficient
Suction surface
Nusselt's number

1. INTRODUCTION

Gas turbine nozzle guide vanes necessitate cooling at elevated temperatures to achieve high thermal efficiency and specific work output. However, the need for more suitable materials capable of withstanding such conditions poses a challenge. The designer used various cooling techniques to keep the blade at a safe limit. The film cooling technique is one such technique that is widely used, employing secondary fluid (coolant) through film cooling holes, which offers a viable cooling solution. Film cooling, a method utilized in hot-gas-path components, is effective for cooling but reduces thermal efficiency due to mixing cool injection gas with hot gases in the main flow, causing aerodynamic losses. Various studies have investigated loss mechanisms in turbomachinery flows, concluding that the mechanism depends on the coolant injection method and location (Han et al., 2012). A few studies from the literature related to the impact of coolant injection on aerodynamic losses are reported here.

Early studies, such as those by Hartsel (1972) and Ito et al. (1980), explored the aerodynamic losses associated with different cooling techniques, highlighting the importance of coolant injection methods and their impact on downstream pressure losses. They found that total pressure losses can increase or decrease on the downstream side of the coolant injection. Similarly, Day et al. (1997, 1998, 2000) performed the aerodynamic analysis experimentally. They concluded that suction surface film cooling reduced aerodynamic efficiency. Fan shaped holes exhibited more aerodynamic losses compared to the cylindrical holes by showing broad and deeper wakes than the cylindrical holes. Stephan et al. (2010) did experimental work to investigate the influence of film cooling on aerodynamic losses by injecting the coolant at the pre-throat and post-throat of a first-stage high-pressure NGV with trailing edge ejection. They concluded that the aerodynamic losses incurred due to the increase in coolant mass flow rate are more than the increase in film cooling effectiveness. These studies underscore the complex interplay between coolant flow dynamics and aerodynamic efficiency in NGVs. According to the experiments of Saha et al. (2013) on both suction and pressure surfaces, they concluded that the suction surface holes mainly influenced the losses compared to the pressure surface. The aerodynamic

Nomenclature

C	vane chord	RANS	Reynolds Averaged Navier Stokes
d	diameter of film hole	TPLC	Total Pressure Loss Coefficient
h	surface heat transfer coefficient	r	diffusion coefficient
K	thermal conductivity	Ø	variable
k	turbulence kinetic energy	S	source term
Kf	thermal conductivity of mainstream	T	temperature
L	length of the hole	U	velocity
Lc	length of vane chord	Y	distance
μ	kinematic Viscosity	**Subscripts**	
M	blowing ratio (B.R.)	C	coolant
NGV	Nozzle Guide Vane	G	mainstream
Nu	Nusselt's number	Oi	total inlet
Poi	total inlet pressure	Oe	total exit
Poe	total exit pressure	f	film

losses were more sensitive to the blowing ratio than to the film cooling holes' row position.

Researchers such as Lanzillotta et al. (2017) and Kim et al. (2023) have demonstrated that film cooling holes' location and blowing ratio significantly influence the aerodynamic performance and cooling effectiveness. Higher blowing ratios, while beneficial for film adherence, can lead to increased total pressure losses and diminished cooling efficiency due to jet lift-off and mixing with the mainstream flow. The challenge lies in balancing these factors to achieve optimal cooling without compromising the aerodynamic performance of the NGV.

The effect of injection at the mid-chord region on the suction side (throat region) decreased the film cooling effectiveness by increasing blowing ratios. According to the experimental studies of Yao et al. (2021), the suction surface was the most effective part after the leading edge, considering the heat transfer coefficient, and suggesting cooling on the suction surface. Denser coolant decreased the Nu number due to the less interaction between the coolant and mainstream, which reduced the injection momentum.

Some other recent literature was also mentioned below related to the suction surface injection. He et al. (2019) numerically investigated the aerodynamic and film cooling performance of a gas turbine NGV of a GE-E3 engine and cylindrical holes, which have less total pressure losses than the trenched holes at high blowing ratios. From the experimental and numerical studies of Dawei et al. (2023), the pressure surface showed lesser total pressure losses due to a lower mass flow rate and coolant velocity than the suction surface. Gao et al. (2018) conducted experiments to investigate the impact of coolant injection near the suction surface throat of a high-pressure turbine vane cascade, combined with trailing-edge ejection. Injection of the coolant at the suction surface increased the boundary layer thickness, and the wake region shifted downstream of the suction surface. The wake peak increased slightly compared to the vane without injection. The addition of trailing edge ejection to the suction surface coolant injection further increased the wake peak, thickened the wake region, and shifted the wake downstream of the pressure surface. However, the study did not include an evaluation of thermal performance. Gudla and Pujari (2025) experimentally investigated the film cooling characteristics of the pressure and suction surfaces of the NGV at different cooling row locations. According to them, the ingestion of the mainstream at the post-throat region of the suction surface film cooling rows decreased the overall film cooling performance under different mass flow ratios. From the above studies it was identified that the post-throat region of the NGV suction surface is a critical area while considering both aerodynamic and film cooling performance.

Investigations on the trailing edge portion have also been carried out in the past years to achieve both aerodynamic and film cooling performance. Yeranee and Rao (2023) worked on a wedge-shaped channel representing a gas turbine trailing edge to investigate the thermal and aerodynamic performance. The Gyroid structures were compared with the pin fin for the study. The tip of the wedge shape is kept open to pass the coolant out of the wedge. Even if the heat transfer is enhanced at the trailing edge, the pressure loss and cooling performance cannot be satisfied with the internal cooling technique. Pujari (2019) numerically investigated the internal surface temperature distribution for a combined impingement-cooled nozzle guide vane. According to their research, they concluded that generalized geometries were not suitable for accurate predictions. So, studies on the whole nozzle guide vane geometry give better results while estimating the life of the nozzle guide vane.

Uzol and Camci (2001) studied the aerodynamic performance on the trailing edge of a turbine blade with different coolant ejection rates for a subsonic flow field. The studies were conducted for trailing edges without cut-back lengths. At a low ejection rate, coolant (up to 3%) showed more total pressure losses due to the mixing of the coolant with the mainstream. There was a reduction in the losses with an increase in the ejection rate of 5%. Aminossadati and Mee (2013) investigated the aerodynamic performance of a gas turbine nozzle guide vane with coolant ejection at the trailing edge with different spanwise inclined slots (0 to 45 degrees). The total pressure loss was minimal at low coolant to mainstream mass flow rate ratios (<1.5%) for all inclined slot angles.

Du et al. (2021) reviewed the heat transfer characteristics at the trailing edge of gas turbine components. Their study highlights the trailing edge as the most thermally and aerodynamically sensitive region of the blade or vane. To minimize aerodynamic losses, the trailing edge must be kept thin, which results in a highly complex flow structure characterized by shock and expansion waves, unsteady vortex shedding, and boundary layer transitions—factors that contribute to elevated heat loads. Additionally, the uneven temperature distribution between the pressure and suction surfaces induces significant thermal stresses, often leading to premature failure. Consequently, effective cooling of the trailing edge is both critical and challenging. Liu et al. (2025) conducted both experimental and numerical studies on a trailing edge cut-back film cooling structure and studied the vortices formation at different blowing ratios along with the film cooling effectiveness. However, the complete analysis of aerodynamic studies was not performed.

Yildiz et al. (2024) optimized the aerothermal performance of film cooling hole placements on the squealer tip of a high-pressure turbine blade, using the total pressure loss coefficient to evaluate aerodynamic performance. Zhang et al. (2025) numerically investigated the aero-thermal aspects of the first-stage nozzle guide vane of the GE-E3 Engine under different non-uniformities at the inlets. The non-uniformities include swirls and hot streaks. Due to the non-uniformities of the heat transfer coefficient, film cooling performance was affected. Kukutla and Prasad (2019) analysed the aerothermal aspects of an impingement-film cooled NGV to optimize the film hole diameters. One dimensional flow network approach was used for the study.

From the above literature survey, it is observed that many researchers have extensively examined the aerodynamic losses' impact on film cooling, investigating factors such as coolant injection methods, hole configurations, blowing ratios, and coolant locations. However, there is a need for a deeper understanding of how these parameters collectively influence the overall aerodynamic efficiency of NGVs, particularly in the post-throat region of the suction surface. While numerous studies have explored either aerodynamic losses or film cooling effectiveness individually, there is a lack of integrated analysis considering both aspects simultaneously. Further, it is observed that in the trailing edge region, there remains a gap in research focusing on the trailing edge's aerodynamic performance concerning coolant ejection rates, slot angles, and their impact on total pressure losses. In this paper, the authors explored aerodynamic losses and effectiveness results at various blowing ratios for cylindrical holes.

Despite substantial advancements in understanding the impact of film cooling on NGV performance, gaps remain in the literature concerning the integrated effects of different blowing ratios and hole configurations on both aerodynamic and thermal characteristics. Previous studies have often focused on the aerodynamic losses or the cooling effectiveness in isolation. There is a need for comprehensive investigations that consider both aspects simultaneously to develop more efficient cooling strategies for high-pressure turbine components.

Based on the literature review, it is evident that considerable research has been conducted on trailing edge ejection and cut-back length in gas turbine blades. However, the complete elimination of trailing edge ejection and adding a row of trailing edge film cooling holes on the suction surface (downstream of the throat) was not reported in the literature. Furthermore, none of the researchers reported both film cooling effectiveness and aerodynamics losses together. In this study, this gap in current research is addressed by investigating both the aerodynamic and thermal performance of the nozzle guide vane. Moreover, optimizing blowing ratios and hole configurations to enhance cooling efficiency without compromising aerodynamic performance remains a complex challenge, offering valuable insights for the development of advanced cooling systems in gas turbine engines

2. COMPUTATIONAL METHODOLOGY

2.1 Computational Domain

A high-pressure gas turbine first-stage Nozzle guide vane with film cooling holes is selected for the present investigation. The geometrical details of the NGV are given in Table 1. SS2 set of holes was placed at the post throat region on the suction side. Details are given in Table 2. ANSYS SPACE CLAIM was used to create the computational domain with both fluid (Mainstream and coolant) and solid regions, as shown in Fig. 1. Periodic boundary conditions were used for the top and bottom walls. Coupled boundary conditions were used for the solid and fluid interactions with solid material of thermal conductivity 0.18 W/mK. The detailed boundary conditions are shown in Table 3

Table 1 Specifications of the NGV

Vane chord	177mm
Pitch	150mm
Pitch Chord ratio	0.84
Staggered angle	54°
Span of the vane	100mm
Exit blade angle	72°

Table 2 Film holes specification

Film hole Row Number	No. of film holes	Diameter of the film hole (mm)	Streamwise Inclination	Span wise Inclination	Pitch/Diameter (P/d)
SS2	17 (Above) 12 (Below)	1.8	70 degree	No	2.7

Table 3 Boundary conditions for the computational study

Mainstream Inlet	Velocity inlet
Coolant inlet	Mass flow inlet
Mainstream outlet	Pressure outlet
The temperature of the Mainstream	318K
Temperature of the coolant	303K
Turbulence intensity	5%
Blowing ratios	0.69,1.07,1.67,2.06
Density ratio	1.01
Reynolds' Number Range	51000 to $1.43x10^5$

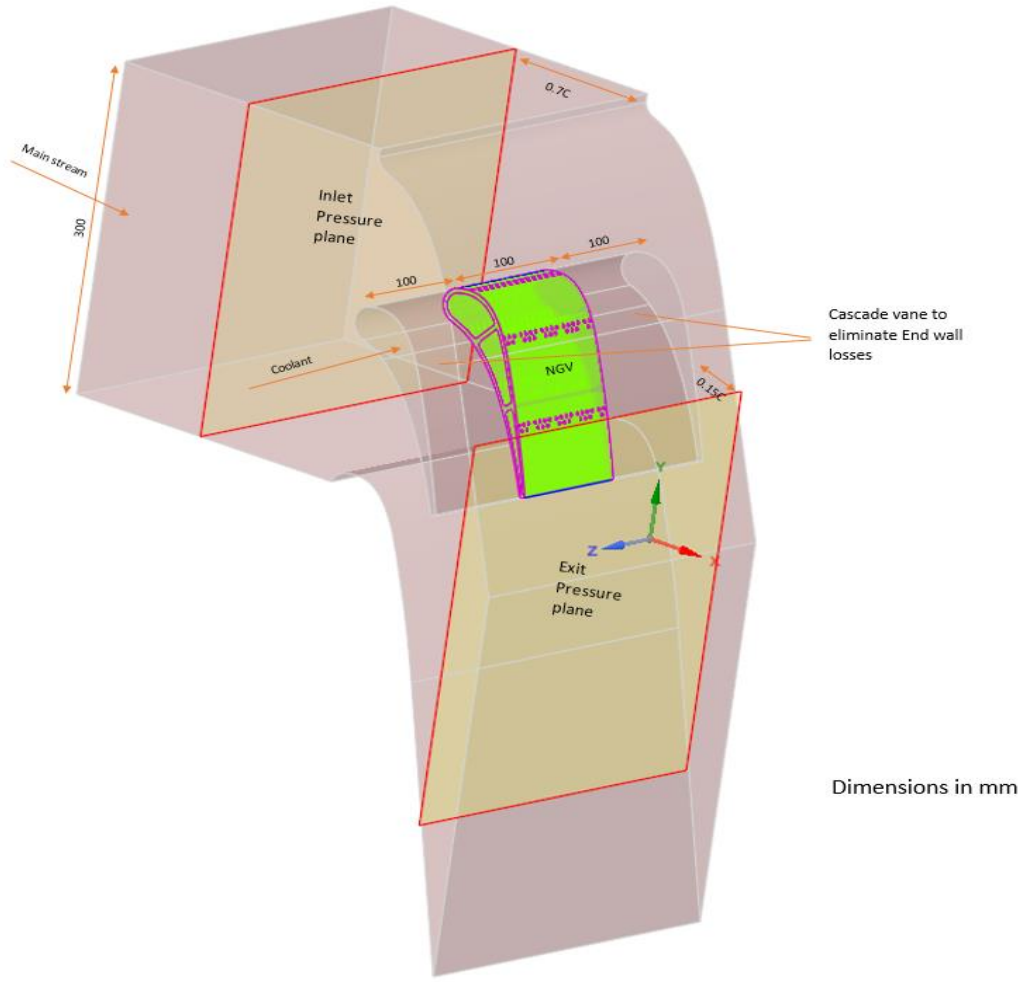

Fig. 1 Computational domain with nomenclature including inlet and exit planes

Computational work has been carried out using the ANSYS Fluent software to achieve the objectives of the present work. A fluent Meshing tool was used to generate the mesh and obtain the grid points. The combination of structured (Hexacore &Polyhedral) and unstructured (Tetrahedral) mesh elements was used in generating the mesh, as shown in Fig. 2. The non-dimensional y+ value (Eq. 1) of 2.1 was maintained on the NGV for the FINE mesh. Twenty-five prism layers were created near the solid and mainstream fluid interface regions to capture fluid flow near the boundary layers. Similarly, five prism layers were generated in the film hole region to capture the fluid flow at the boundaries inside the holes. Figure 3(a) shows the film cooling layout of the SS2 film holes that were placed at the post throat of the suction surface.

$$y+=\frac{u\Delta y\rho}{\mu} \tag{1}$$

2.2 Grid Independence Study

Grid convergence was studied for all three types of mesh, according to Celik et al. (2008). The graph is plotted for the effectiveness with respect to the span of the vane at the exit of the film holes rows SS1 at the blowing ratio (M) of 0.64 along the line AB (Fig. 3(b)), as shown in Fig. 4. GCI for fine mesh is the value of 0.0044, which gives the discretization error of the numerical study.

Table 4 Mesh details for grid Independence study

Type of Mesh	No. of Cells	Area-averaged film cooling effectiveness.	Relative Change (%)
COARSE	3237867	0.657	-
MEDIUM	7574623	0.668	1.67
FINE	16641611	0.667	0.15

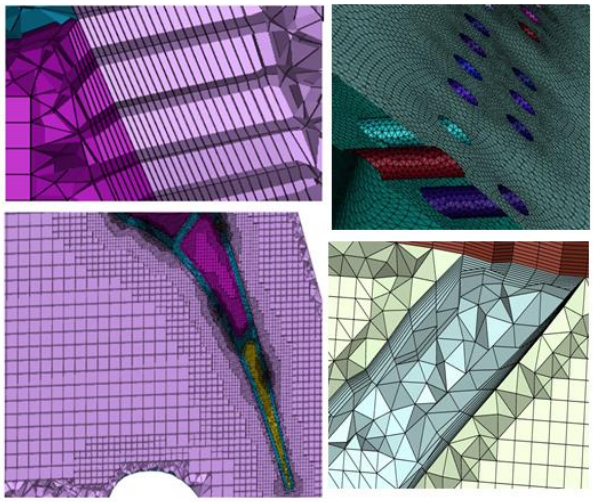

Fig. 2 Mesh generated for the simulation work

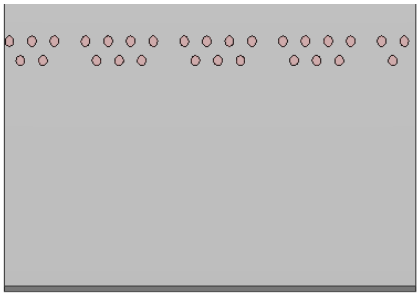

(a)

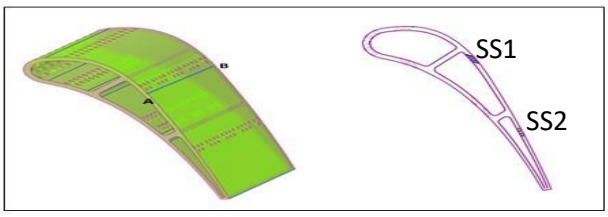

(b)

Fig. 3 SS2 Film cooling holes layout used for the present study (a) and Nozzle guide vane with film cooling holes without trailing edge ejection(Distorted view) (b)

According to Celik et al. (2008). The fine grid convergence index is given by the Eq. (2)

$$GCI_{fine}^{21} = \frac{1.25e_a^{21}}{r_{21}^p - 1} \quad (2)$$

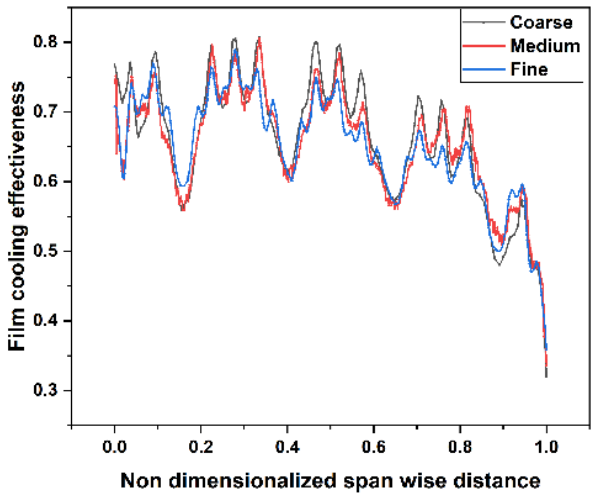

Fig. 4 Film cooling effectiveness for Line AB along the spanwise distance

Where, e_a is called the approximate relative error, p is the apparent order, and r_{21} is the grid refinement factor for coarse to fine mesh.

The other sources of numerical errors include modelling errors due to the assumptions taken in the turbulence models, boundary conditions, and simplifications in the geometry.

A grid independence test was conducted by considering three different mesh sizes (coarse, medium, and fine), and the convergence data is shown in Table 4. The least relative change of 0.15% was obtained in the fine mesh, and therefore, the fine mesh was considered for the simulations. Convergence criteria of 10^{-5} were considered for continuity, momentum, turbulence models, and energy equations. Solution is converged monotonically.

2.3 Governing Equations

RANS equations were solved using the finite volume method to obtain the results. Turbulence equations were also solved along with mass, momentum, and energy equations. k ω turbulence model with shear stress transport (SST) equation was used as a turbulence model for solving the turbulence equation. The turbulence model was selected for its proven effectiveness in capturing separation and boundary layer behaviour, offering better reliability than alternative models. Pressure and velocity are coupled by the SIMPLE algorithm, and a second-order upwind scheme is used to discretize continuity, momentum, energy, and turbulence equations. The following assumptions were taken while solving the governing equations (Eq. 3).

Table 5 Geometrical and flow parameters of published experimental and present computational works

Geometrical and flow parameters	Experimental work (Ramesh et al., 2017))	Present Computational work
Material Thermal conductivity	0.18 W/mK	0.18 W/mK
L/d	4	5.2
s/d	3	2.7
Blowing Ratio	2	2
The temperature of the Mainstream	297K	297K
Temperature of the coolant	323K	323K
Mass flow of the coolant	0.00357kg/s	0.00357kg/s
Vane axial chord	0.1336m	0.1046m

1) Flow is incompressible
2) Flow is considered to be steady
3) No radiation and natural convection effects
4) Constant fluid properties

$$\frac{\partial \emptyset}{\partial t}+\frac{\partial (u\emptyset)}{\partial x}+\frac{\partial (v\emptyset)}{\partial y}+\frac{\partial (w\emptyset)}{\partial z}=\frac{\partial}{\partial x}\left[\Gamma\frac{\partial \emptyset}{\partial x}\right]+\frac{\partial}{\partial y}\left[\Gamma\frac{\partial \emptyset}{\partial y}\right]+\frac{\partial}{\partial z}\left[\Gamma\frac{\partial \emptyset}{\partial z}\right]+S_{\emptyset} \quad (3)$$

By substituting the required variables in the above equation, continuity, momentum, and energy equations are obtained.

Continuity equation:

$\emptyset=1;\ r=0;\ S_{\emptyset}=0$

Momentum:

$\emptyset= u, v, w;\ \Gamma=\nu+\nu_T;$

$$S_{\emptyset}= -\frac{1}{\rho}\frac{\partial p}{\partial x}+S'u, -\frac{1}{\rho}\frac{\partial p}{\partial y}+S'v, -\frac{1}{\rho}\frac{\partial p}{\partial z}+S'w$$

Energy:

$$\emptyset=T;\ r=\frac{V}{Pr}+\frac{V_T}{Pr_T};\ S\emptyset=S_T$$

$$\text{Blowing Ratio M}=\frac{(\rho V)jet}{(\rho V)mainstream} \quad (4)$$

$$\text{Total pressure loss coefficient (TPLC)}=\frac{P_{oi}-P_{oe}}{P_{oi}-P_{se}} \quad (5)$$

$$\text{Film cooling effectiveness } \varepsilon=\frac{T_g-T_f}{T_g-T_c} \quad (6)$$

$$\text{Nusselt's Number, Nu}=\frac{hL_c}{K_f} \quad (7)$$

$$h(x)=\frac{q\,(x)}{Tf(x)-Tr(x)} \quad (8)$$

The reference temperature (T_r) is considered the mainstream temperature of the flow.

2.4 Validation of Computational Study with the Published Experimental Work (Ramesh et al., 2017):

Experiments by Ramesh et al. (2017) on the nozzle guide vane were considered to validate the computational results. The single-row holes at the mid-suction surface of the present author's NGV profile were used for comparison. The laterally averaged effectiveness at a blowing ratio of two was chosen for validation. Table 5 shows the geometrical and flow parameters of the experimental work (Ramesh et al., 2017) and presents computational work. The reason for the deviation is the change in the leading edge profile of the present configuration, and Ramesh et al. (Fig. 5) is quite different. The variation in the L/d and S/d ratios and the difference in the axial chord of the two profiles also affect the deviation. The combined standard uncertainty was found to be 5.5%. The comparison is shown in Fig. 5.

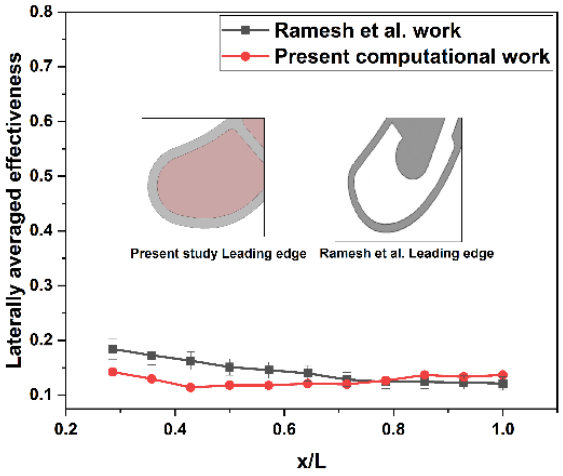

Fig. 5 Comparison of computational work with Ramesh et al. (2017) work

3. RESULTS AND DISCUSSION

3.1 Effect of the Blowing Ratio on the Film Cooling Performance

The impact of the blowing ratio on the film cooling performance of nozzle guide vanes (NGVs) is extensively analysed in this section.

Detailed contour maps of the film cooling effectiveness for four blowing ratios (0.69, 1.07, 1.67, and 2.06) are shown in Fig. 6.

Higher film effectiveness is observed near the film hole and it decreased in the downstream region. However, at higher blowing ratio it is observed that the film effectiveness is decreasing. This is due to decrease in mainstream Reynolds number and increase in jet momentum. At blowing ratio of 0.69, film cooling is effective nearer to the film holes as compared to other blowing ratios. This confirmed that higher mainstream velocity can increase the film formation, but it does not significantly improve film cooling effectiveness. This is because the coolant's momentum is used to counteract flow separation losses rather than to improve cooling performance.

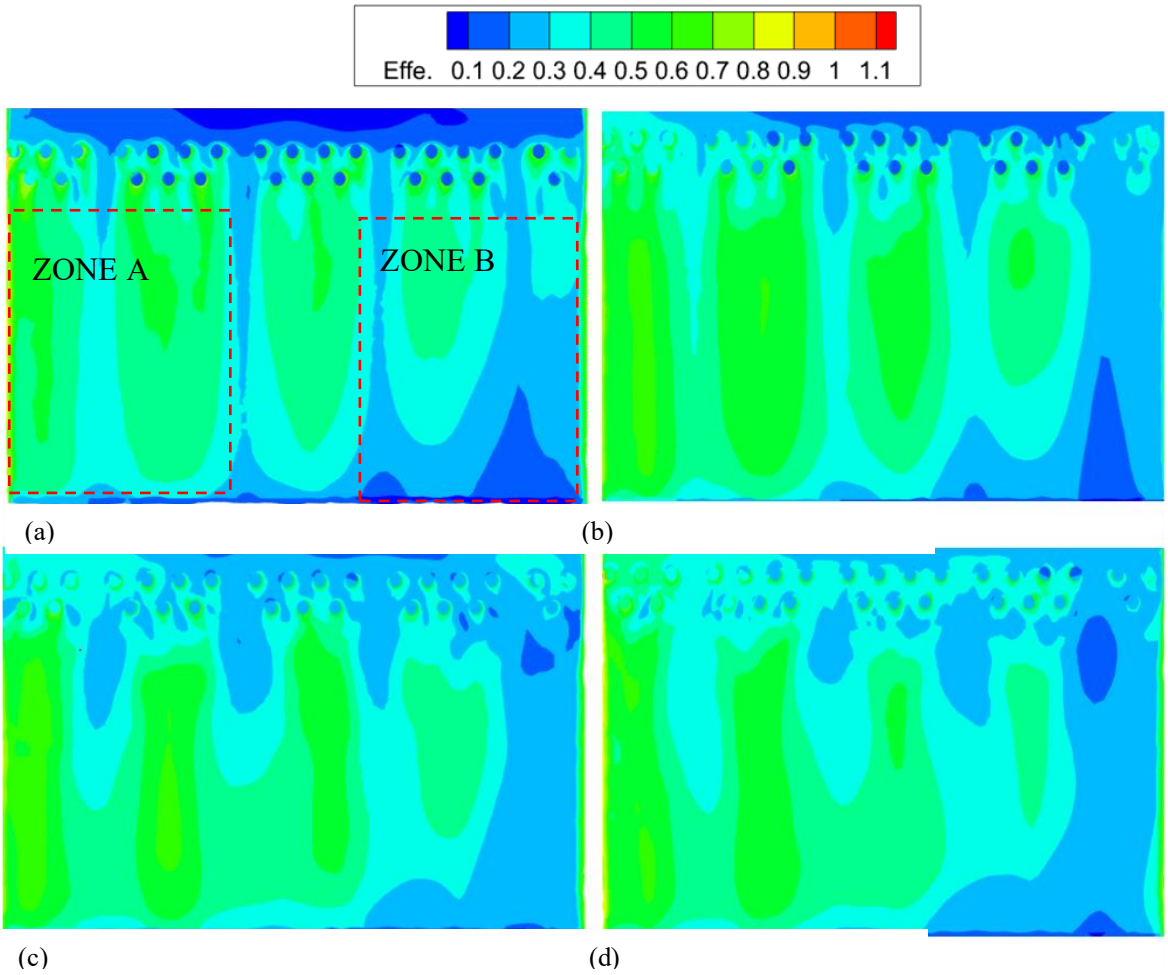

Fig. 6 Film cooling effectiveness contours of the trailing edge region for the blowing ratios a) M=0.69, b) M=1.07, c) M=1.67, d) M=2.06

The analysis showed that film cooling effectiveness depends on hole position and blowing ratio. At a blowing ratio of 0.69, the upper row (SS2) outperformed the lower row in effectiveness due to a higher coolant mass flow. Increasing the blowing ratio to 2.06 caused partial film formation on the ZONE B, due to reduced pressure difference. In contrast, better film coverage and effectiveness on the ZONE A side resulted from flow separation and higher pressure gradients. Negative pressure gradients in the post-throat region lead to increased boundary layer thickness and a higher tendency for flow separation as blowing ratios rise. This promotes higher mixing between the coolant jet and mainstream flow at higher blowing ratios, reducing film cooling effectiveness. Additionally, the interaction between the coolant jet and mainstream generates counter-rotating vortex pairs (CRVPs).

As mainstream velocity increases, these vortices enhance lateral coolant spreading, improving film coverage and cooling effectiveness at lower blowing ratios. The streamlined pattern for the blowing ratio of 1.67 is shown on the non-dimensional velocity contour in Fig. 7.

The graph in Figure 8 shows the area-weighted averaged film cooling effectiveness of the film-cooled area at different blowing ratios. Initially, the effectiveness increased from a low blowing ratio 0.69 and

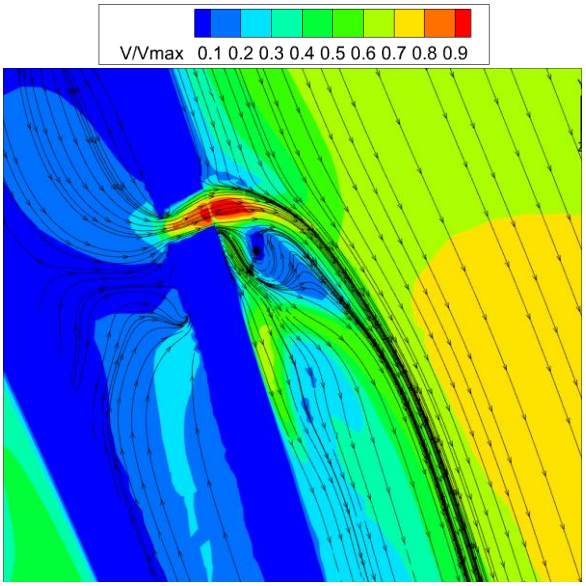

Fig. 7 Streamline pattern and velocity contours for the centre plane at M=1.67

slightly increased with 18% rise from 1.07 to 2.06. Later, the percentage increase in effectiveness from 1.67 to 2.06 was only 1.45%. The drop in percentage is due to the higher jet lift off and mixing of coolant with the mainstream.

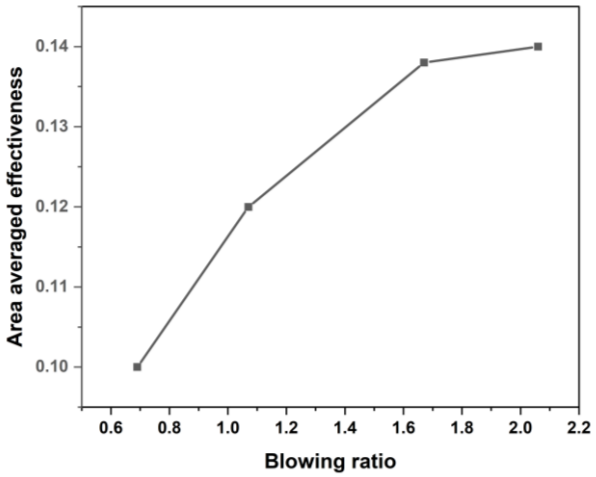

Fig. 8 Graph between the area-averaged film cooling effectiveness of the film-cooled area vs. the blowing ratio

The Fig. 9 shows laterally averaged effectiveness along the stream wise distance for all the four different blowing ratio. At blowing ratio 0.69 the avg. effectiveness decreases along the stream wise distance. However, same trend is not observed for the remaining three blowing ratio. This is because the blowing ratio is varied by varying the mainstream Reynolds number and by keeping the coolant flow constant. This causes the non-uniform distribution of the film along the stream wise direction. this effectiveness decreases as the blowing ratio increases. At a blowing ratio of 1.07, the cooling performance is greater in the middle region of the trailing edge because the reattachment of the film is taking place in the specified region. However, at higher blowing ratios (1.67 and 2.06), the effectiveness did not significantly improve and started to diminish at the trailing edge.

In summary, it is observed that moderate blowing ratios optimize film cooling by keeping the coolant attached to the surface, maximizing thermal protection. Excessive blowing ratios reduced the effectiveness due to jet lift-off and mixing. These findings are key for designing efficient cooling in high-temperature turbine components.

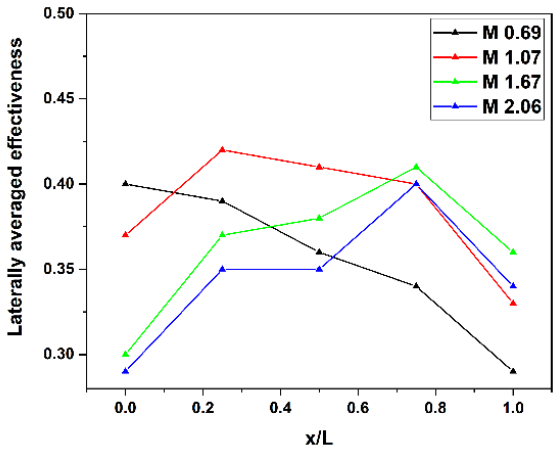

Fig. 9 Graph between Laterally averaged effectiveness Vs stream wise distance at different blowing ratios

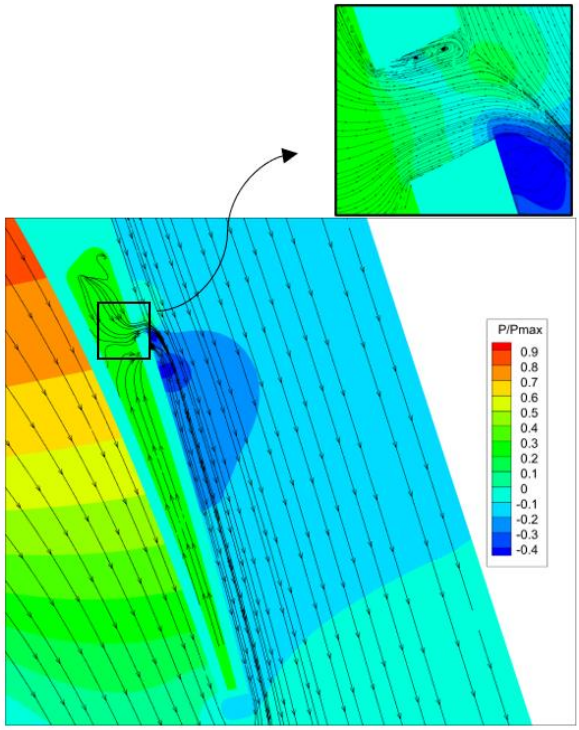

Fig. 10 Streamlines and static pressure contour of the center plane at M=0.69

3.2 Streamlines and Pressure Contours at the Center Plane

The study of streamlines and pressure contours at the center plane provides insightful visualization of film formation on the vane surface for various blowing ratios (B.R.). The plane was chosen so that the middle part of the cooling hole (upper row of the SS2) is visible. The streamlines in the trailing edge region and the static pressure distribution in the background illustrate how different blowing ratios impact the flow and film effectiveness.

3.2.1 Blowing Ratio (B.R.) = 0.69

The center plane of the post-throat region of the nozzle guide vane (NGV) is illustrated in Fig. 10. Both pressure contours and streamlines are depicted, showing that the mainstream and coolant flow smoothly and adhere closely to the vane surface. This behavior is due to the low velocity and momentum of the coolant jet. However, the film formed has a lower effectiveness, which is attributed to mixing the mainstream and coolant inside the film hole. It can be seen in the Fig. 10 film holes' region. A negative pressure region near the film hole, followed by gradual pressure recovery toward the trailing edge, indicates that this blowing ratio has a minimal effect on exit pressure loss.

3.2.2 Blowing Ratio (B.R.) = 1.07

With a higher blowing ratio of 1.07 as shown in Fig. 11, the increased momentum of the coolant jet facilitates the formation of a more effective film than B.R. = 0.69. The coolant and mainstream mixing within the film holes is reduced, leading to a slight reattachment observed immediately

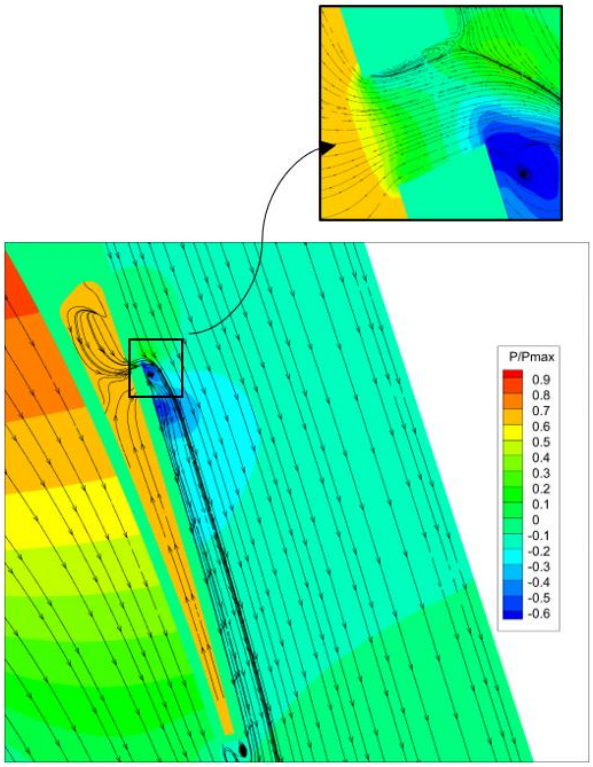

Fig. 11 Streamlines and static pressure contour of the center plane at M=1.07

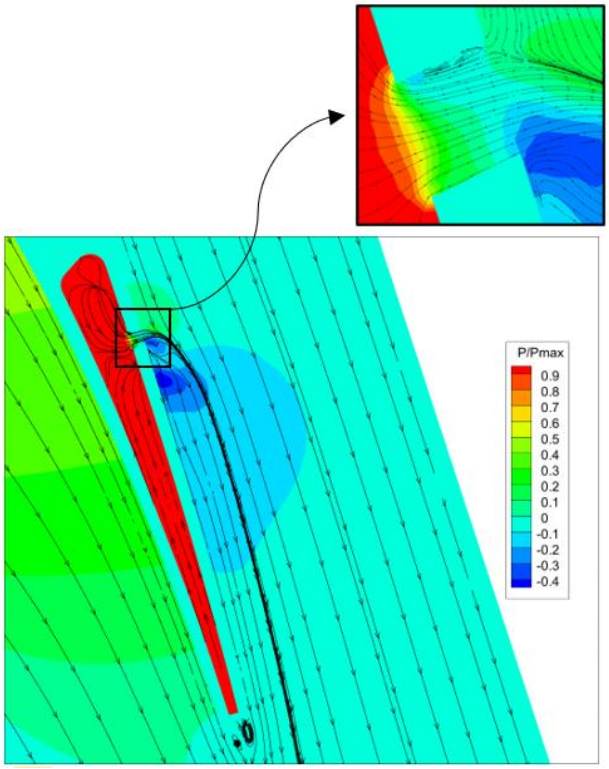

Fig. 12 Streamlines and static pressure contour of the center plane at M=1.67

at the film hole exit because of the higher jet velocity. Additionally, vortices are formed at the negative pressure region near the film hole exit. The pressure recovery is better than that at B.R. = 0.69, resulting in greater film effectiveness and increased total pressure loss.

3.2.3 Blowing Ratio (B.R.) = 1.67

Figure 12 shows the streamlines for the blowing ratio 1.67. The B.R. has a more significant effect on the static pressure recovery than increasing the film effectiveness. The higher pressure in the coolant plenum chamber and film hole causes a noticeable lift-off on the suction surface near the film hole exit. The momentum of the coolant jet at this ratio is greater than that at B.R. = 1.07, which can be seen in the streamline patterns near the vane suction surface in Fig. 12. Lift-off indicates less coolant film attachment to the vane surface.

3.2.4 Blowing Ratio (B.R.) = 2.06

At the highest blowing ratio of 2.06 which is shown in the Fig. 13, the coolant jet mixes thoroughly with the mainstream, which prevents the formation of a continuous film. However, the film reattaches to the vane surface after a certain distance. No negative pressure is observed at the film hole exit, and the streamlines indicate a smooth flow pattern. The flow pattern and pressure distribution for B.R. = 2.06 are similar to those observed at B.R. = 1.67 (Fig. 12), showing a consistent trend at higher B.R.s.

In summary, the analysis of streamlines and pressure contours reveals that as the blowing ratio increases, the effectiveness of the coolant film and the pressure recovery on the vane surface improve up to a certain point. A lower

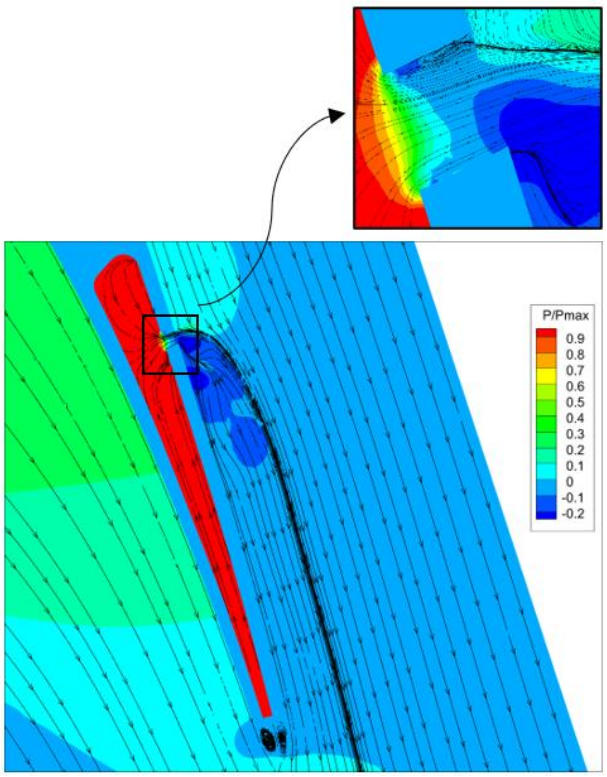

Fig. 13 Streamlines and static pressure contour of the center plane at M=2.06

blowing ratio (B.R. = 0.69) results in less effective film formation and minimal impact on exit pressure loss, whereas higher ratios (B.R. = 1.67 and 2.06) enhance

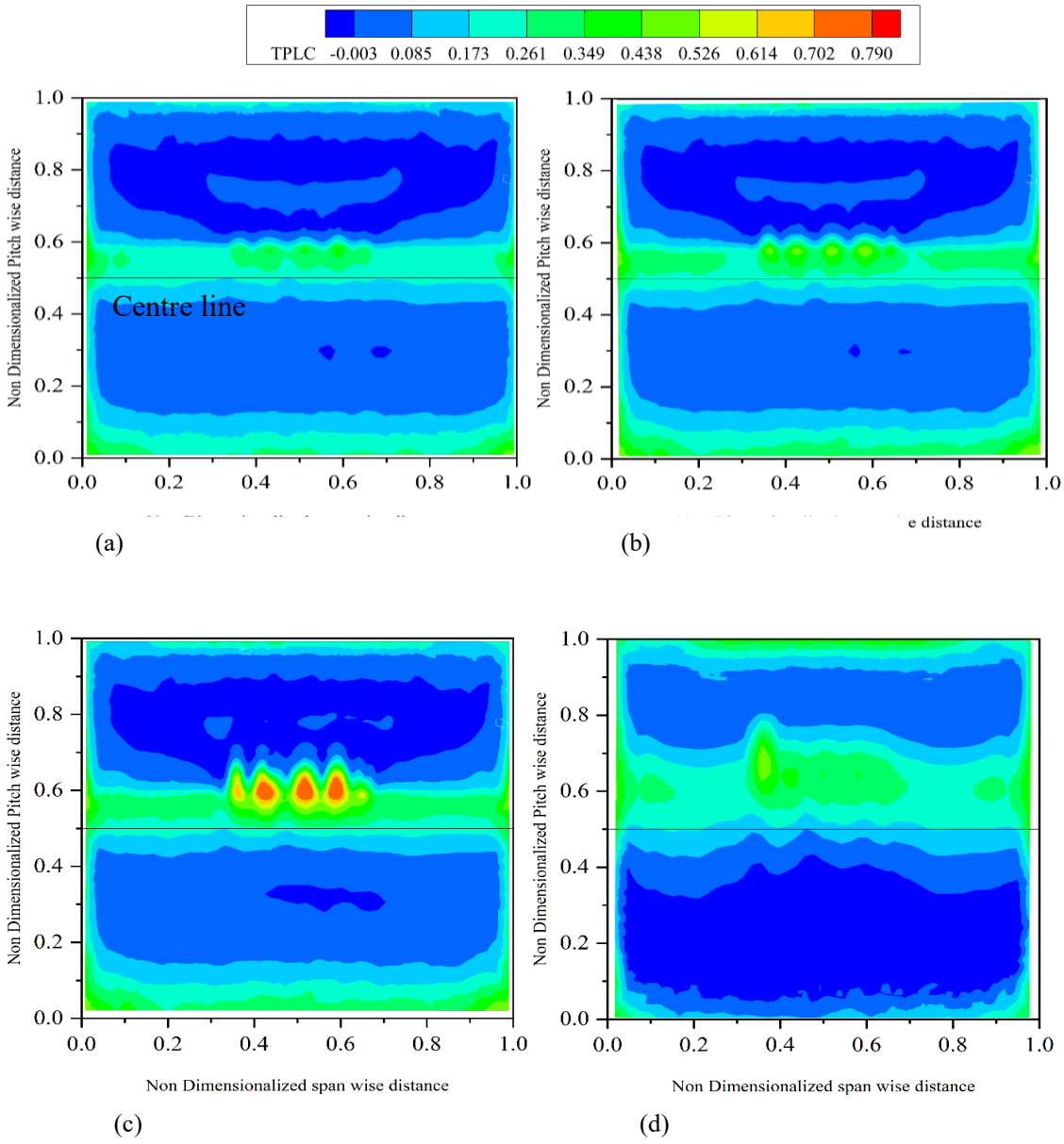

Fig. 14 Total pressure losses at exit plane for a) M=0.69, b) M=1.07, c) M=1.67, d) M=2.06

pressure recovery but may cause the film to lift from the vane surface. The flow dynamics and effectiveness of the coolant film are significantly influenced by the coolant jet's momentum and mixing behavior with the mainstream.

3.3 Effect of Blowing Ratio on Total Pressure Loss Coefficient (TPLC)

This section analyses how blowing ratios affect total pressure loss in a vane cascade at the exit plane. The exit pressure plane was taken at a distance of 0.15 times the chord length from the vane trailing edge. From Fig. 14, at M=0.69, TPLC at the exit is low and uniformly distributed, indicating efficient mixing and low losses. As the ratio increases to M=1.07, pressure slightly drops and becomes more uneven (at a center line), signalling rising mixing losses. As the suction side has lower pressure than the pressure side, the TPLC distribution shows a similar trend at the exit plane as well. (Can be seen in the pitch wise direction TPLC in the Fig. 14.)

At a blowing ratio of M=1.67, the total pressure loss coefficient further decreased, particularly toward the suction surface, and the losses are greater at the central trailing edge region. This indicates that higher blowing ratios enhance the mixing of the coolant with the mainstream flow, leading to increased pressure losses. The high-pressure loss region also shifted slightly from the centre line toward the suction surface, suggesting the effects of jet lift-off and increased film momentum. When the blowing ratio reaches 2.06, the total pressure loss significantly decreases, with a highly nonuniform distribution by reducing negative pressure gradients. This reduced the flow separation, particularly under subsonic conditions.

Figure 15 shows how the blowing ratio affects the area weighted average total pressure loss coefficient. As the blowing ratio increases, the loss coefficient also rises, reaching a peak at a blowing ratio of 1.67. Beyond this

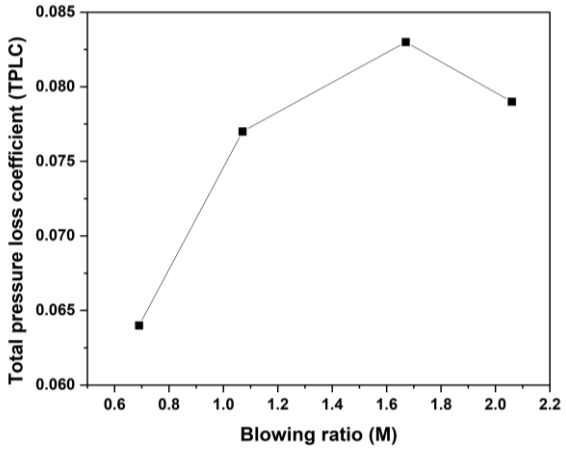

Fig. 15 Graph between area-weighted average Total pressure loss coefficient vs. blowing ratio

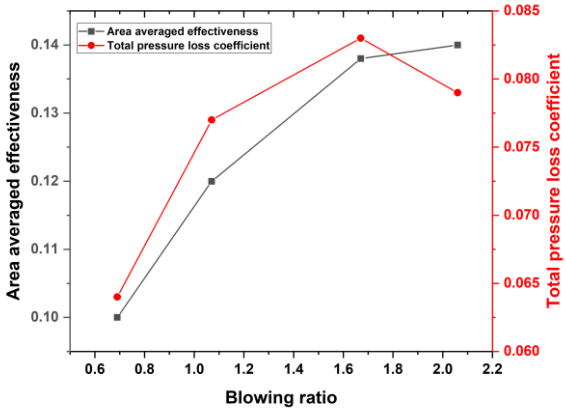

Fig. 16 Combined graph showing area-weighted effectiveness and total pressure loss coefficient at different blowing ratios

point, the coefficient decreases. The initial increase is due to higher coolant flow and poor mixing between the coolant and the mainstream, which raises total pressure loss. However, at blowing ratios above 1.67, the coolant jet lifts off, leading to better mixing with the mainstream and temperature uniformity, resulting in reduced pressure loss at the exit.

Similarly, Fig. 16 presents a combined plot of the total pressure loss coefficient and area-averaged film cooling effectiveness across various blowing ratios. Both effectiveness and pressure loss coefficient increase with blowing ratio up to 1.67. Beyond this point, the effectiveness begins to decline gradually, as indicated by a reduced slope in the effectiveness curve. In contrast, the total pressure loss coefficient drops sharply after 1.67. Therefore, blowing ratio 1.67 is considered as the optimum value in view of both aerodynamic and film cooling point of view.

3.4 Effect of the Blowing Ratio on the Nusselt Number:

The Nusselt number is a key dimensionless quantity in heat transfer analysis, representing the ratio of convective to conductive heat transfer across a boundary. Understanding the thermal performance of systems where

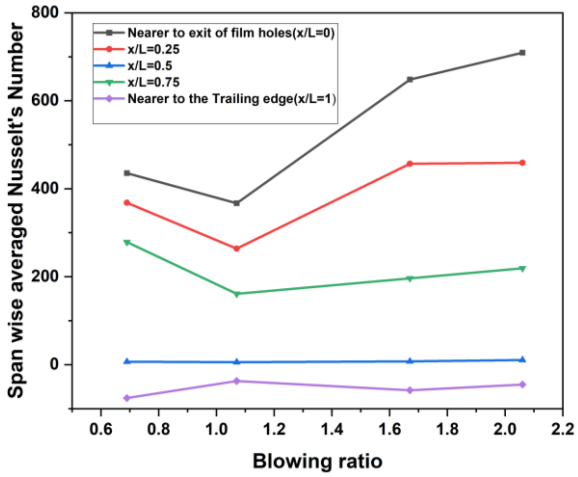

Fig. 17 Graph between spanwise line average Nu number and Blowing ratio between the exit of the film holes and the trailing edge along the streamwise distance

fluid flows over surfaces is essential. Figure 17 shows the impact of the blowing ratio on the Nusselt number, specifically focusing on the heat transfer coefficients in the post-throat region of the suction surface under constant heat flux conditions.

Spanwise line-averaged Nusselt numbers were taken at different positions between the exit of the film holes and the trailing edge of the post-throat region. The mainstream temperature is the reference point for these calculations, and the results are non-dimensionalized via the Nusselt number. This normalization allows for a comparison of heat transfer performance under different blowing ratios.

The graph in the Fig. 17 indicates that the Nusselt number is highest near the film hole exit and decreases as the distance from the film holes increases. This trend is due to the temperature difference between the film surface and the mainstream being most significant near the film holes and diminishing in the streamwise direction up to the trailing edge. At the trailing edge, a negative Nusselt number is observed because heat is transferred from the film to the mainstream due to the mixing of the two fluids.

At a blowing ratio of 1.07, a thicker boundary layer forms on th vane surface than at a blowing ratio of 0.69, resulting in a lower heat transfer coefficient. Higher blowing ratios increase the momentum of the coolant jet, increasing its mixing with the mainstream.

Moreover, it increases the heat transfer coefficient. The favorable pressure gradient increases with increasing jet momentum, leading to a steep increase in the Nusselt number at higher blowing ratios, as shown in Fig. 17. Notably, at 50% distance from the film holes, the Nusselt number remains nearly constant across different blowing ratios, likely due to the similar temperature differences between the film and mainstream.

3.5 Comparison of the Trailing Edge Film-Cooled Vane with the Trailing Edge Ejected Vane

The total pressure loss coefficient (TPLC) of the trailing edge (TE) film-cooled vane is compared with that

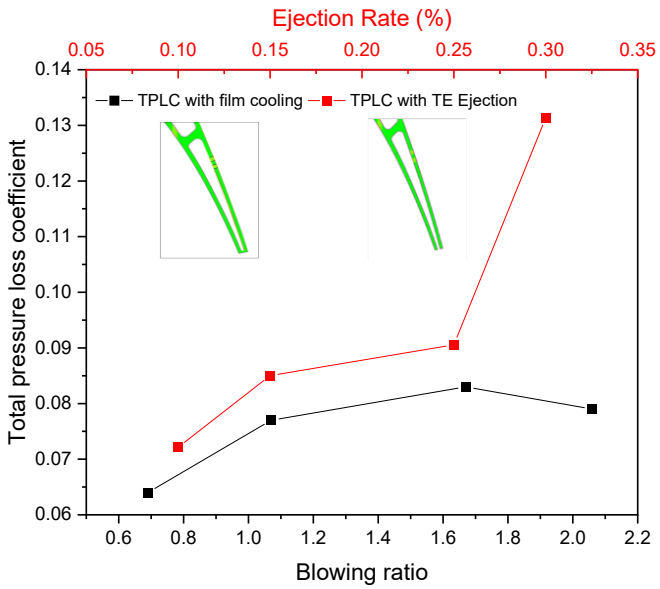

Fig. 18 Area averaged total pressure loss coefficient at the exit plane of the NGV with film cooling at the Trailing edge and with Trailing Edge Ejection

of a nozzle guide vane (NGV) utilizing traditional TE ejection without film cooling. As shown in Figure 18, eliminating TE ejection and instead incorporating film cooling holes on the post-throat suction surface leads to a reduction in the TPLC compared to the NGV with TE ejection. The graph presents the variation in TPLC for different blowing ratios in the film-cooled vane and for varying ejection rates in the TE ejection configuration. The coolant mass flow rates and main stream velocities used in both configurations are equivalent, allowing for a direct comparison. In the film cooling configuration, the post-throat region is cooled via surface injection, which alters the pressure loss characteristics. The higher losses observed in the TE ejection case are attributed to the direct and more disruptive coolant mixing with the mainstream flow. In contrast, film cooling results in localized mixing, which reduces the flow's momentum near the trailing edge and minimizes overall flow disturbances, leading to a lower TPLC. The loss coefficient decreased by 20% by replacing the TE ejection with the new film cooling hole rows on the suction side.

Additionally, as shown in the figure, an increase in the ejection rate increased the TPLC, and there is an abrupt increase in the loss coefficient above 0.25% ejection rate for the TE ejection case. The results of the TE ejection followed a similar trend to the studies of Uzol and Camci (2001).

4. CONCLUSIONS

In conclusion, this study provides a detailed analysis of the aero-thermal performance of a nozzle guide vane (NGV) equipped with a novel film cooling configuration, which replaces traditional trailing-edge ejection with two rows of cooling holes. The results demonstrate that the blowing ratio significantly influences both aerodynamic and thermal behavior. Notably, the momentum of the coolant jet plays a critical role in enhancing film cooling effectiveness while also contributing to increased total pressure losses.

1. Lower blowing ratios are found to be more effective in maintaining the film attachment and minimizing total pressure losses, while higher blowing ratios, although enhancing the coolant jet momentum, led to increased mixing losses and reduced cooling effectiveness due to jet lift-off.
2. From B.R. 0.69 to 1.67, The area averaged Total pressure loss coefficient raised by 31.25%. Later, from 1.67 to 2.06, It reduced by 8.93%.
3. Similarly, From B.R. 0.69 to 1.67, The area averaged effectiveness increased by 35%. From 1.67 to 2.06, the effectiveness increased by 3.3%.
4. The blowing ratio 1.67 can be considered as the optimum value in view of both film cooling performance and aerodynamic losses.
5. 20% decrease in loss coefficient at the exit plane is achieved by replacing the TE ejection with the film cooling on the post throat area of the suction surface, i.e., a new film cooling configuration.
6. Choosing the minimum coolant mass flow rate for a given mainstream mass flow rate leads to film formation on the vane surface. When the mainstream flow velocities are lower and the coolant jet velocities are higher, it causes higher jet lift-off, causing reduced pressure losses and film effectiveness under subsonic conditions. The jet lift-off can be reduced, and better film attachment can be obtained by increasing the mainstream velocity. Therefore, both coolant and mainstream mass flow rates are crucial in determining the optimal blowing ratio, and CFD analysis is essential in order to predict the optimized blowing ratio.

CONFLICT OF INTEREST

The authors have no conflicts of interest in publishing this article.

AUTHORS CONTRIBUTION

Babji Gudla: Methodology, Investigation, Data Curation, Formal analysis, Writing –original draft; **Arun Kumar Pujari:** Conceptualization, Supervision, Funding acquisition review and editing.

REFERENCES

Aminossadati, S. M., & Mee, D. J. (2013). An experimental study on aerodynamic performance of turbine nozzle guide vanes with trailing-edge spanwise ejection. *Journal of Turbomachinery*, *135*(3). https://doi.org/10.1115/1.4006663

Celik, I. B., Ghia, U., Roache, P. J., Freitas, C. J., Coleman, H., & Raad, P. E. (2008). Procedure for estimation and reporting of uncertainty due to discretization in CFD applications. *Journal of Fluids Engineering, Transactions of the ASME, 130*(7), 0780011–0780014. https://doi.org/10.1115/1.2960953

Dawei, C., Qiang, D., Qingzong, X., Guangyao, X., Haoyang, L., & Hongye, L. (2023). Film cooling and aerodynamic loss performance of turbine vanes with fan-shaped and wave-trenched holes. *Applied Thermal Engineering, 230*. https://doi.org/10.1016/j.applthermaleng.2023.120643

Day, C. R. B., Oldfield, M. L. G., Lock, G. D., & Dancer, S. N. (1998). *Efficiency Measurements of an Annular Nozzle Guide Vane Cascade With Different Film Cooling Geometries.* Proceedings of the ASME 1998 International Gas Turbine and Aeroengine Congress and Exhibition. Volume 4: Heat Transfer; Electric Power; Industrial and Cogeneration. Stockholm, Sweden. June 2–5, 1998. V004T09A088. ASME. https://doi.org/10.1115/98-GT-538

Day, C., Oldfield, M. & Lock, G. (2000) Aerodynamic performance of an annular cascade of film cooled nozzle guide vanes under engine representative conditions. *Experiments in Fluids 29*, 117–129. https://doi.org/10.1007/s003489900062

Day, R. C. R. B., Oldfield, M. L. G., & Lock, G. D. (1997). *The Influence of Film Cooling on the Efficiency of an Annular Nozzle Guide Vane Cascade*. http://asmedigitalcollection.asme.org/GT/proceedingspdf/GT1997/78682/V001T03A104/2408543/v001t03a104-97-gt-521.pdf

Du, W., Luo, L., Jiao, Y., Wang, S., Li, X., & Sunden, B. (2021). Heat transfer in the trailing region of gas turbines – A state-of-the-art review. *Applied Thermal Engineering*, *199*. https://doi.org/10.1016/j.applthermaleng.2021.117614

Gao, J., Wei, M., Liu, Y., Zheng, Q., & Dong, P. (2018). Experimental and numerical investigations of hole injection on the suction side throat of transonic turbine vanes in a cascade with trailing edge injection. Proceedings of the Institution of Mechanical Engineers, *Part G: Journal of Aerospace Engineering, 232(8),* 1454–1466. https://doi.org/10.1177/0954410017694918

Gudla, B., & Pujari, A. K. (2025). Influence of film cooling row locations on the thermal performance of nozzle guide vanes: an experimental study. *Heat Transfer Research*, *56*(8), 73–94. https://doi.org/10.1615/HeatTransRes.2025056945

Han, J. C., Dutta, S., & Ekkad, S. (2012). *Gas Turbine Heat Transfer and Cooling Technology*. Second Edition. CRC Press.

Hartsel, J. E. (1972). *Prediction effects of mass-transfer cooling on the blade row efficiency of turbine airfoils*. AIAA 10th Aerospace science meeting, January 17-19, California, AIAA.

He, W., Deng, Q., Zhou, W., Gao, T., & Feng, Z. (2019). Film cooling and aerodynamic performances of a turbine nozzle guide vane with trenched cooling holes. *Applied Thermal Engineering, 150*, 150–163. https://doi.org/10.1016/j.applthermaleng.2019.01.002

Ito, S., Eckert, E. R. G., & Goldstein, R. J. (1980). Aerodynamic loss in a gas turbine stage with film cooling. http://www.asme.org/about-asme/terms-of-use

Kim, G. M., Jeong, J. Y., Kang, Y. J., & Kwak, J. S. (2023). Comparison of aerodynamic loss of a gas turbine vane with various trailing edge cooling schemes. *Aerospace, 10(2).* https://doi.org/10.3390/aerospace10020143

Kukutla, P. R., & Prasad, B. V. S. S. S. (2019). *Fluid thermal network studies on cooled nozzle guide vane.* Proceedings of the ASME 2019 Gas Turbine India Conference. Volume 1: Compressors, Fans, and Pumps; Turbines; Heat Transfer; Structures and Dynamics. Chennai, Tamil Nadu, India. December 5–6, 2019. V001T03A014.ASME. https://doi.org/10.1115/GTINDIA2019-2651.

Lanzillotta, F., Sciacchitano, A., & Rao, A. G. (2017). Effect of film cooling on the aerodynamic performance of an airfoil. *International Journal of Heat and Fluid Flow, 66,* 108–120. https://doi.org/10.1016/j.ijheatfluidflow.2017.05.011

Liu, J., Wang, P., Wang, P., Liu, J., Du, Q., Wang, H., Wang, Z., Shen, X., & Zhu, J. (2025). Experimental and numerical study on the trailing edge cut-back cooling characteristics with POD analysis. *Journal of Thermal Science*, *34 (3).* https://doi.org/10.1007/s11630-025-2024-6

Pujari, A. K. (2019). CFD study of combined impingement and film cooling flow on the internal surface temperature distribution of a vane. *International*

Journal of Turbo and Jet Engines. https://doi.org/10.1515/tjj-2019-0010

Ramesh, S., LeBlanc, C., Narzary, D., Ekkad, S., & Alvin, M. A. (2017). Film cooling performance of tripod antivortex injection holes over the pressure and suction surfaces of a nozzle guide vane. *Journal of Thermal Science and Engineering Applications*, *9*(2). https://doi.org/10.1115/1.4035290

Saha, R., Fridh, J., Fransson, T., Mamaev, B. I., & Annerfeldt, M. (2013). *Suction and pressure side film cooling influence on vane aero performance in a transonic annular cascade.* Proceedings of the ASME Turbo Expo. 6. https://doi.org/10.1115/GT2013-94319.

Stephan, B., Kru¨ ckels, J. R., & Gritsch, M. (2010). *Investigation of aerodynamic losses and film cooling effectiveness for a ngv profile.* GT2010-22810 Power for land, sea and air. http://proceedings.asmedigitalcollection.asme.org/pdfaccess.ashx?url=/data/conferences/gt2010/70457/

Uzol, O., & Camci, C. (2001). Aerodynamic loss characteristics of a turbine blade with trailing edge coolant ejection: Part 2- External aerodynamics, total pressure losses, and predictions. *Journal of Turbomachinery*, *123*(2), 249–257. https://doi.org/10.1115/1.1351817

Yao, C. Y., Zhang, Z., Zhang, B. L., & Zhu, H. R. (2021). Heat transfer characteristic of a fully cooled turbine vane. *Case Studies in Thermal Engineering, 28.* https://doi.org/10.1016/j.csite.2021.101547

Yeranee, K., & Rao, Y. (2023). Turbulent flow and heat transfer enhancement for turbine blade trailing edge cooling with gyroid-type triply periodic minimal surfaces. *Journal of Engineering for Gas Turbines and Power, 145*(7). https://doi.org/10.1115/1.4062157

Yıldız, F., Alpman, E., Kavurmacıoğlu, L., & Camci, C. (2024). Aerothermal optimization of film cooling hole locations on the squealer tip of an HP turbine blade. *Journal of Thermal Science and Engineering Applications* *16*(5), 051001. https://doi.org/10.1115/1.4064431

Zhang, S., Ding, S., Qiu, T., Liu, C., & Gan, C. (2025). Numerical investigation on aerothermal performances of film cooled high pressure turbine vane under inlet non-uniformities. *International Journal of Heat and Mass Transfer*, *237*. https://doi.org/10.1016/j.ijheatmasstransfer.2024.126398